Piled up gravitational waves: Searching for new signals of Nnaturalness

Paul Archer-Smith, Dylan Linthorne, and Daniel Stolarski
Ottawa-Carleton Institute for Physics, Carleton University,
1125 Colonel By Drive, Ottawa, Ontario K1S 5B6, Canada *

We explore the possibility of detecting gravitational waves generated by 1st order phase transitions in multiple dark sectors. Nnaturalness is taken as a sample model that features multiple additional sectors, many of which undergo phase transitions that produce gravitational waves. We examine the cosmological history of this framework and determine the gravitational wave profiles generated. These profiles are checked against projections of next generation gravitational wave experiments, demonstrating that Nnaturalness can indeed produce unique gravitational wave signatures that will be probed by these future experiments.

I. INTRODUCTION

II. GRAVITATIONAL WAVES

Sectors other than the SM can be reheated through multifield inflationary theories, Reheaton models, etc. In these models, the SM will receive the majority of the energy density while the remaining energy density will be distributed, in a model dependent way, to the various hidden sectors. If there does not exist a portal between the sectors, they will remain decoupled and evolve independently. When looking at multiple thermally decoupled hidden sectors it is convienent to define the temperature ratio [cite cold,dark,noisy]

$$\xi_i \equiv \frac{T_i}{T_\gamma} \tag{1}$$

Where T_i is the temperature of the i^{th} hidden sector, and T_γ the temperature of the standard model (assuming radiation domination).

- first order phase transitions (strength, scale, origin) Right after reheating, the temperatures of the respective sectors are high leading to restoration of a given sector's symmetry. An example being the SM's $SU(3) \times SU(2) \times U(1)$ symmetry being restored as the scalar potential's vev becomes global minimum. As the sectors cool down their scalar potentials may change, producing a new global vev at which the symmetry will break by an induced phase transition. Depending on the characteristics of the symmetry breaking, the phase transition may be strongly first ordered (SFOPT).

Once the temperature reaches the critical temperature the SFOPT will occur, at which bubbles of the new phase will start to nucleate. These bubbles will expand, eventually colliding and merging until the entire sector is within the new phase. These bubbles are discribed by the following Euclidean action

$$S_E(T) = \frac{1}{T}\int d^3x \left[\frac{1}{2}(\nabla\phi)^2 + V(\phi, T)\right] \tag{2}$$

Where the time component has been integrated out due to finite temperature effects. The system has solutions with a $O(3)$ symmetry. We leave the thermalized potential $V(\phi, T)$ general, since an exact QCD potential at the time of the chiral phase transition is not well understood. Some authors have used the chiral effective lagrangian to calculate a low energy thermalized potential for confining $SU(N)$.

The amount of energy density dumped into the individual sectors dictates the energy budget for the PT and hence for the gravitational waves. A quantity that characterizes the strength of the PT is the ratio of the latent heat and energy density of radiation, at the time of nucleation,

$$\alpha = \frac{\epsilon}{g_* \pi^2 (T_\gamma^{nuc})^4/30} \tag{3}$$

Assuming that there is a negligible amount of energy being dumped back into the SM radiation bath, which would cause significant reheating of ρ_γ, the latent heat of the PT ϵ should approximately be the energy density of the hidden sector going through the PT. g_* has weak temperature dependence in a single sector, but when dealing with multiple hidden sectors, g_* gains contributions from all N sector's relativistic degrees of freedom, weighted by their respective temperature ratios (energy densities).

$$g_* = g_{*,\gamma} + \sum_{i=1}^{N} g_{*,i}(\xi_i)^4 \tag{4}$$

It will be seen that for models with a significant number of hidden sectors, that the lack of substantial reheating in adjecent sectors will cause their respective g_* corrections to become negligible, $g_* \approx g_{*,\gamma}$.

* PaulSmith3@cmail.carleton.ca

III. PARTICLE SETUP

Beginning with the work of Pedro Schwaller [1] and continuing through the work of many others [**?**], strong first order phase transitions for SU(N) dark sectors with arbitrary numbers of flavours have been explored as a source of gravitational waves. Here, we look to generalize this study to include classes of models that feature multiple dark sectors that undergo gravitational wave producing phase transitions. The multiple sets of gravitational waves produced in these types of models superimpose: potentially creating signals that deviate from the typical phase transition gravitational wave spectrum. For any multi dark sector model, the behaviour of the QCD phase transition for each sector must be understood — sectors that feature a weak cross-over transition do not generate the sought after gravitational wave signatures. We use Nnaturalness as an example framework since it features N distinct QCD sectors at a wide range of possible scales; this allows us to probe a wide range potential signature of this class of models. As an additional bonus, different sectors ("standard" and "exotic", as will be outlined later in this section) can lead to different types of symmetry breaking outlined in Sec. IV.

A. NNaturalness

Nnaturalness is a model framework that looks to solve the hierarchy problem through the introduction of N mutually non-interacting sectors [2]. The framework itself is very general: the various sectors can possess a wide range of particle content that can be freely selected by the model builder. The one exception to this is that "our" sector must consist of the Standard Model. For simplicity, the original paper takes all additional new sectors to be copies of the SM (with the same gauge groups and Yukawa structure); however the Higgs mass parameters of each sector are allowed to taken on values distributed between $-\Lambda_H^2$ and Λ_H^2, with Λ_H being the scale that cuts off quadratic divergences.

This construction leads to sectors that are automatically accidentally tuned to the $1/N$ level, leading to a sector with a mass parameter $m_H^2 \sim \Lambda_H^2/N$. The sector with the smallest non-zero vacuum expectation value (vev) as "our" sector — the SM sector. It should be noted that the values of m_H^2 pass through zero, resulting in effectively 2 types of sectors: "standard" sectors like our own with a negative Higgs mass parameter squared, possess a vev, and exhibit electroweak symmetry breaking and "exotic" sectors with a positive Higgs mass parameter squared that thus feature no electroweak symmetry breaking and a zero vev.

Keeping with the original convention, we write our mass parameter as

$$\left(m_H^2\right)_i = -\frac{\Lambda_H^2}{N}(2i + r), \tag{5}$$

where i denotes the sector ($-\frac{N}{2} \leq i \leq \frac{N}{2}$). $i = 0$ is the sector that possess the smallest vev and is thus "our" SM sector. Finally, the parameter r is a way to adjust the tuning of the model: adjusting r away from 1 (which leads to purely uniform spacing) allows us to make a larger gap between our sector and the next one. Within this work, we looked at variants on this sort of tuning including non-uniform distributions and clustered sector effects; these ideas are discussed in Sec. VI.

As mentioned above, half of all sectors in this model feature a Higgs mass parameter such that $m_H^2 < 0$. These sectors feature electroweak symmetry breaking just like in the SM, however the vevs produced scale with the changing mass parameter: $v_i \sim v\sqrt{i}$. As the masses for particles in these sectors scale with the vev, this leads to the masses of particles within each sector strictly increasing with i. The consequences of this on the QCD of $i \geq 1$ sectors is further discussed in Sec. IV.

The remaining sectors within this model provide a radical departure from our own. $m_H^2 > 0$ leads to no vev and electroweak symmetry is only broken at very low scales due to the phase transition from free quarks to confinement at the QCD scale Λ_{QCD}. As a result, fermion masses are produced via four-fermion interactions generated after integrating out the SU(2) Higgs multiplet. This leads to very light fermions: $m_f \sim y_f y_t \Lambda_{QCD}^3/(m_H^2)_i \leq 100$ eV, with y_f representing the Yukawa coupling to fermion f. The extremely light quarks that appear in these sectors dramatically change the nature of the QCD phase transition — unlike the SM, the transition is strongly first order. Again, this is further developed in Sec. IV. Crucially, this results in the production of gravitational waves. This is the physical signature we're interested in exploring within this paper; the calculation and results are presented in Sec. VI.

B. Reheating N Sectors

A key issue within Nnaturalness is how to predominantly gift energy density to our own sector so as to not be immediately excluded by number of effective neutrinos (N_{eff}) bounds. This is done through the introduction of a post-inflationary field called the "reheaton". After inflation, the reheaton field possess the majority of the energy density of the Universe. Although this field can generically be either by bosonic or fermionic, we reduce our scope to a scalar reheaton ϕ. Our focus is primarily the production of gravitational waves from multiple sectors: the shifting to a fermion reheaton doesn't change the scaling of the energy density of the exotic sectors and, as a result, is ignored in our analysis.

In order to maintain the naturalness of our SM sector, the reheaton coupling is taken to be universal to every sector's Higgs. However, a large amount of the Universe's energy density must ultimately be deposited in our own sector for Nnaturalness to avoid instant exclusion. In order to accomplish this the decay width into each sector

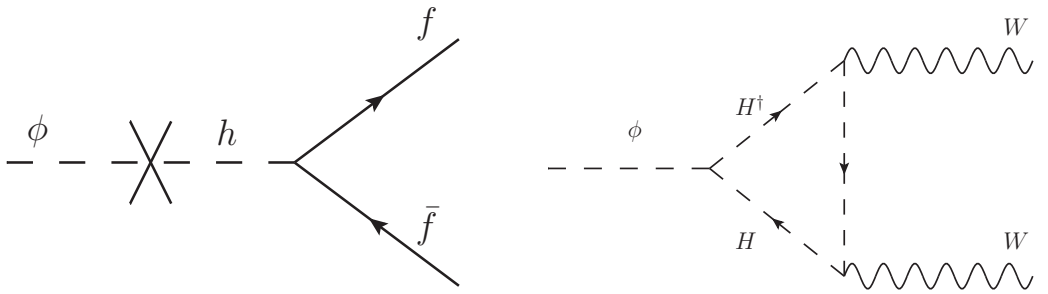

FIG. 1. Feynman diagrams for primary reheaton decays assuming $m_\phi \ll m_H$. The left decay is the primary decay for standard sectors ($\langle H \rangle \neq 0$), with f representing all possible fermions. The right decay occurs in exotic sectors ($\langle H \rangle = 0$)

must drop as $|m_H|$ grows. If we insist that the reheaton is a gauge singlet that is both the dominant coupling to every sector's Higgs and lighter than the naturalness cutoff $\Lambda_H/\sqrt{N}$ then we construct a model that behaves as desired.

Ultimately, after examining the gravitational wave case produced by standard Nnaturalness, we generalize our results to include the (rather unnatural) case where sectors are reheated "randomly" as opposed to in relation to the higg's mass parameter. This allows us to explore more general models with multiple dark sectors at a huge range of scales. For these models, the reheating mechanism remains undefined and the results of this section are completely irrelevant.

The appropriate Lagrangian for a scalar reheaton ϕ is:

$$\mathcal{L}_\phi \supset -a\phi \sum_i |H_i|^2 - \frac{1}{2} m_\phi^2 \phi^2. \tag{6}$$

Note that the cross-quartic couplings are absent, suppressed by a very small coupling. Effective Lagrangians for the two different types of sectors present in this theory can be obtained through the integrating out of the Higgs bosons in every sector:

$$\begin{aligned} \mathcal{L}_\phi^{v\neq 0} &\supset C_1 a y_q \frac{v}{m_h^2} \phi q q^c, \\ \mathcal{L}_\phi^{v=0} &\supset C_2 a \frac{g^2}{16\pi^2 m_H^2} \phi W_{\mu\nu} W^{\mu\nu}, \end{aligned} \tag{7}$$

with C_i representing numerical coefficients, g the weak coupling constant, and $W^{\mu\nu}$ the SU(2) field strength tensor.

Immediately from Eq. (7), we can see that the matrix element for decays into standard sectors is inversely proportional to that sectors higgs mass, $\mathcal{M}_{m_H^2<0} \sim 1/m_{h_i}$. The Feynman diagram for this process is presented in Fig. 1. The loop decay of $\phi \to \gamma\gamma$ is always sub-leading and can be neglected. It should be noted that as one goes to sectors with larger and larger vevs, the increasing mass of the fermions eventually leads to situations where the decay to two on-shell bottom or charm quarks is kinematically forbidden, $m_\phi < 2m_q$. For sectors where this kinematic threshold is passed for charm quarks, contributions to cosmological observables can be safely ignored. All in all, we end up with a decay width that scales as $\Gamma_{m_H^2<0} \sim 1/m_h^2$. Since we can expect energy density to be proportional to the decay width, $\frac{\rho_i}{\rho_{SM}} \approx \frac{\Gamma_i}{\Gamma_{SM}}$, this indicates that energy density of standard sectors falls proportional to $1/i$.

For the exotic sectors, Eq. (7) indicates a matrix element scaling $\mathcal{M}_{m_H^2>0} \sim 1/m_{H_i}^2$. As the Feynman diagram (Fig. 1) shows, the reheaton decays to exotic sectors are loop suppressed, leading to a significantly lower energy density than the standard sectors. Both the decay width and energy density for these sectors scale as: $\Gamma_{m_H^2>0} \sim \rho_i \sim 1/m_H^4 \sim 1/i^2$.

As a final note, the reheating temperature, T_{RH}, has an upper bound on the order of the weak scale. If this bound is not observed, the SM Higgs mass would have major thermal corrections — leading to the branching ratios into other sectors being problematically large. In accordance with this restriction, this project only examines reheating temperatures at or below 100 GeV.

IV. DARK QCD

Due to the confining nature of QCD, the exact nature of the phase transition is often difficult to ascertain analytically and requires the study of lattice simulations. The results of these studies on the nature of QCD phase transitions is summarized in the so-called "Columbia" plot (Fig. 2). As seen in the above figure (and explicitly demonstrated through lattice studies [**?**]), our sector is solidly in the weak-cross over area. In order to observe the strong first order transition required for gravitational wave production, at least some of the additional sectors present must feature quarks in either the heavy quark (pure Yang-Mills) or massless limits.

In the Yang-Mills limit we see $m_{u,d,s} \to \infty$. This leads to the presence of a global Z_3 centre symmetry that is broken at high temperatures but restored low temperatures. Ultimately, this restoration results in a first order phase transition [4]. On the other end of the spectrum,

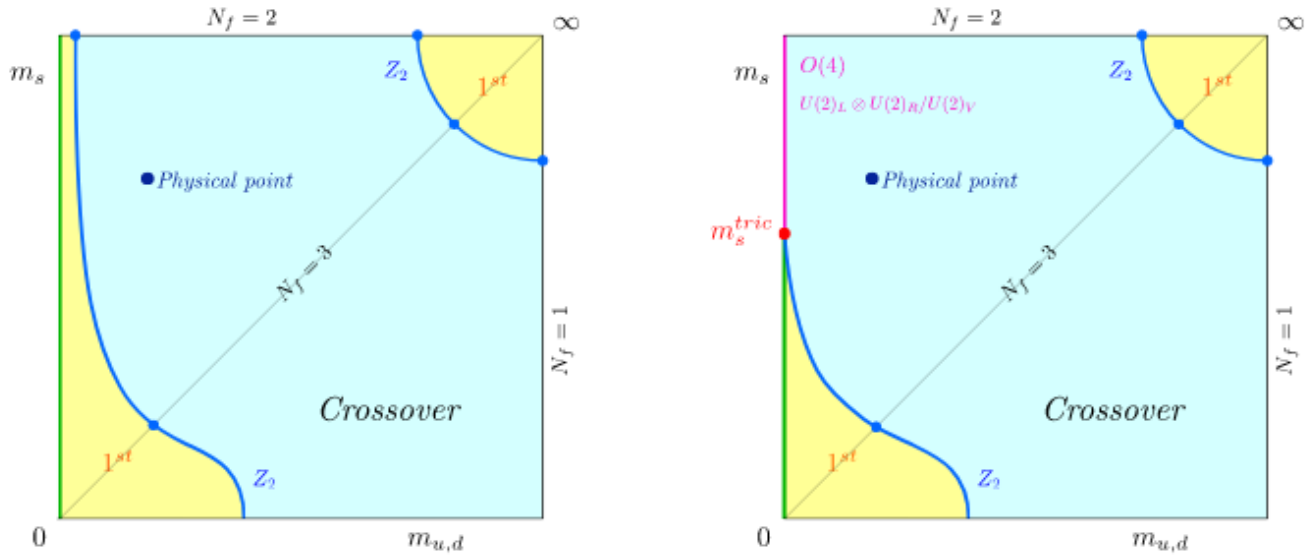

(a) First order scenario in the $m_s - m_{u,d}$ plane

(b) Second order scenario in the $m_s - m_{u,d}$ plane.

FIG. 2. Two possible scenarios for the Columbia Plot with the up and down quark mass taken to be identical. The "physical point" is the Standard Model. Plot from [3]

"massless" quark theories ($m_q \ll \Lambda_{QCD}$ for all quarks) also contain strong phase transitions due to the breakdown of SU(N) × SU(N) chiral symmetry [5]. Both the Yang-Mills and massless limit arguments can be generalized to SU($N \geq 3$): coupling both with the additional restriction that we avoid the conformal window indicates that strong first order phase transitions can occur if we have $n = 0$ (pure Yang-Mills) or $3 \leq n < 4N$ (light quark limit) very light flavours.

For Nnaturalness (or other mirror sector models), standard sectors with higher vevs possess more massive quarks; eventually, sectors with large enough vevs push us into the upper-right corner. Conversely, exotic sectors with zero vev feature incredibly light quarks and drop us into the bottom-left corner. In order to figure out the specifics of each sector, we follow the same procedure as [6] but generalize it to an arbitrary number of additional sectors. First, due to the parameters of each sector being taken to be identical save for the higgs mass squared (thus $v \neq v_i$, where v is the SM vev), we assume that the strong coupling of every sector is identical at some high scale. Explicitly, above the top quark mass scale $\Lambda_{QCD} = 89 \pm 5$ in $\overline{MS}$ [7]. Since the running of the gauge coupling at scale μ is given by

$$\alpha_s(\mu) = \frac{2\pi}{11 - \frac{2n_f}{3}} \frac{1}{\ln \mu/\Lambda} \tag{8}$$

where n_f is the number of quark flavours and Λ is the confinement scale Λ_{QCD} [8].

For any other sector i we write out the expression as:

$$\alpha_s^i(\mu) = \frac{2\pi}{11 - \frac{2n_f^i}{3}} \frac{1}{\ln \mu/\Lambda^i}, \tag{9}$$

featuring the equivalent definitions for the additional sectors. Because we've set the strong couplings equal at high scales, $\Lambda = \Lambda^i$ for all i at scales above the top quark mass for the heaviest sector. However, since the masses of the quarks in each sector are different, we end up with a unique running of the coupling for each sector. At every quark mass threshold for a given sector, we match the coupling strengths above and below the threshold and determine the new Λ^i for the lower scale:

$$\alpha_s^{i(5)} = \alpha_s^{i(6)} \tag{10}$$

and thus

$$\Lambda^i_{(5)} = (m_t^i)^{2/23} (\Lambda^i_{(6)})^{21/23}. \tag{11}$$

Suppressing the is for cleanliness, we can arrive at similar relations at the bottom and charm thresholds

$$\begin{aligned} \Lambda_{(4)} &= (m_b)^{2/25} (\Lambda_{(5)})^{23/25}, \\ \Lambda_{(3)} &= (m_c)^{2/23} (\Lambda_{(4)})^{25/27}. \end{aligned} \tag{12}$$

These can be combined to show that

$$\Lambda_{(3)} = (m_t m_b m_c)^{2/27} (\Lambda_{(6)})^{21/27}. \tag{13}$$

This type of matching procedure can be done as many times as necessary for a given sector. The process terminates when Λ_i for a given scale is larger than the next

quark mass threshold (i.e running the scale down arrives at the Λ_{QCD} phase transition before reaching the next quark mass scale).

In cosmological terms, we can envision a sector's thermal history unfolding where as the plasma cools below each quark mass threshold, said quarks are frozen out. At a certain point, the sector arrives at the QCD phase transition and confinement occurs (provided there are light enough quarks to confine) — if this occurs when ≥ 3 quarks are at a much lower scale or all quarks have already frozen out, we get the desired phase transition.

A. Standard Sectors

As mentioned in the previous sections, for standard sectors with increasing index i the vevs of said sectors increase $v_i \propto \sqrt{i}$. This leads to increasingly heavy particle spectra for higher sectors — eventually leading to sectors that are essentially pure Yang-Mills that featuring strong first order phase transitions. This, of course, begs the question: at what index i do said phase transitions begin?

The actual boundary of region of interest on the Columbia plot is not precisely known and further lattice simulations are required to determine exactly where in parameter space cross-over transitions end and first order transitions begin. In lieu of such studies, we parameterize our ignorance in the form of a "slop factor" κ. Assuming the up and down quarks of each sector to be of roughly the same scale, we determine what sector i features $\kappa m_u^i \approx \Lambda_{QCD}$.

Using the methods outlined in the prior section we determine Λ_{QCD} to have a relevant value of

$$\Lambda^i_{(2)} = (m^i_s m^i_c m^i_b m^i_t)^{2/29} (\Lambda^i_{(6)})^{21/29} \tag{14}$$

at the energy scale we're interested in. $\Lambda^i_{(6)}$ is identical for all sectors and is taken to have a standard model value. Rewriting Eq. (14) in terms of standard model variables,

$$\Lambda^i_{(2)} = (m_s m_c m_b m_t i^2)^{2/29} (\Lambda_{(6)})^{21/29}. \tag{15}$$

Setting this equal to some multiple of the quark mass of sector i,

$$\kappa m^i_u = \kappa m_u \sqrt{i} = (m_s m_c m_b m_t i^2)^{2/29} (\Lambda_{(6)})^{21/29}. \tag{16}$$

This can be solved for i:

$$i = \frac{(m_s m_c m_b m_t)^{4/25} (\Lambda_{(6)})^{42/25}}{(\kappa m_u)^{58/25}}. \tag{17}$$

The critical index demonstrates that even in the most extreme cases, where first order phase transitions occur with the up quark an order of magnitude less than Λ_{QCD}, the critical index is still ~ 1000. Looking back to the description of reheating within Nnaturalness, we see the energy density of these sectors is at most 10^{-4} that of our sector. As a result, the gravitational waves generated by the standard large i sectors in Nnaturalness will not generate detectable signatures.

However, if we move away from the standard Nnaturalness reheating mechanism and begin exploring mirror sectors with large vevs with $\mathcal{O}(> 10\%)$ of our energy density ρ_{SM}, we can have sectors with relatively high dark QCD scales that produce detectable gravitational waves. These sectors feature no baryons and, as such, produce runaway bubbles similar to the exotic sectors in standard Nnaturalness. From Eq. (14) we can determine the confinement scale of an arbitrary mirror sector — the maximum possible given a 10^{16} limit [2] of sectors is $\sim 38\,GeV$. After imposing N_{eff} constraints (as in Sec. V), the energy density of said sector is limited to $\sim 0.25\rho_{SM}$. The signals of this sector and other test cases like it are explored in Sec. VI. It is important to note that these type of sectors mimic the general behaviour of any Yang-Mills like multi dark sector model.

B. Exotic Sectors

In every exotic sector the fermion masses are exceptionally light: even the most massive quark of each sector is orders of magnitude smaller than our confinement scale, $m_t \ll \Lambda_{QCD}$. Additionally, since $m_q \propto 1/(m^2_H)_i$ this separation only becomes more pronounced as we move to sectors further from our own. The scale of the exotic quarks makes it unnecessary to run down the scale of the strong coupling as done for the standard sectors — the phase transition for all exotic sectors occurs at $\sim 90\,\text{MeV}$ and a strong first order phase transition occurs for all exotic sectors at this temperature.

The confinement of these sectors directly leads to the production of both baryons and mesons as we have the spontaneous breaking of $\text{SU}(6) \times \text{SU}(6) \to \text{SU}(6)$. This leads to the production of 35 pseudo-Goldstone bosons during the phase transition. These become relevant in the calculation of gravitational wave signatures through the calculation of the critical phase transition strength, α_∞, with α_∞ denotes the dividing line between the runaway regime ($\alpha > \alpha_\infty$) and the non-runaway regime ($\alpha < \alpha_\infty$). Explicitly [9–11],

$$\alpha_\infty = \frac{(T^{nuc}_h)^2}{\rho_R} \left[\sum_{bosons} n_i \frac{\Delta m_i^2}{24} + \sum_{fermions} n_i \frac{\Delta m_i^2}{48} \right], \tag{18}$$

for particles with n_i degrees of freedom that obtain mass through the phase transition.

The masses obtained through the phase transition can be approximated through the use of a generalization of the Gell-Mann–Oakes–Renner relation [12],

$$m^2_\pi = \frac{V^3}{F^2_\pi}(m_u + m_d), \tag{19}$$

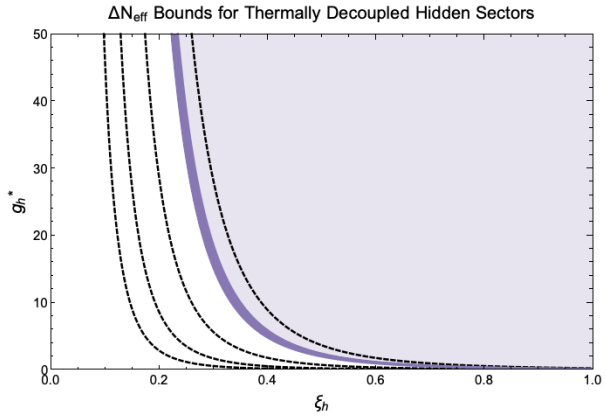

FIG. 3. ΔN_{eff} as a function of relativistic degrees of freedom in a fully decoupled hidden sector (g_h) and the temperature ratio of said sector. Contours set ΔN_{eff} to (0.01, 0.03, 0.1, 0.5) as the dashed lines, from left to right. Most stringent current N_{eff} bounds shade in purple.

where $V \sim \Lambda_{QCD}$, F_π is the pion decay constant. So, for mesons in exotic sector i:

$$m_\pi^i \sim \sqrt{\frac{m_1^i + m_2^i}{m_u + m_d}} m_\pi. \tag{20}$$

Ultimately, calculating the critical phase transition strength for each sector using Eq. (18) indicates that every sector has a phase transition in the runaway regime. Thus, all exotic sectors have strong first order phase transitions that lead to runaway bubble walls.

V. CONSTRAINTS

In general, the multi-hidden sector models explored here feature feature of huge number of (nearly) massless degrees of freedom. Dark photons, neutrinos, and the like abound in these sectors and, assuming a relatively high reheat temperature, the leptons, quarks, and baryons of these sectors are can easily be relativistic. In Nnaturalness this feature is realized quite dramatically: each of the thousands (or millions or billions) of sectors possess relativistic degrees of freedom. The presence of these particles can have two main effects: extra relativistic particles can alter the expansion history of the universe through changes to the energy density or hidden sectors can feature annihilations that reheat the photons or neutrinos of our sector near Big Bang Nucleosynthesis (BBN) and affect the light element abundances. The effective number of neutrino species, N_{eff}, describes these contributions and, as such, is the strictest constraint that must be dealt with when studying these type of multi-phase transition models.

The SM predicts that $N_{eff}^{SM} = 3.046$ [13]. This is in good agreement with bounds from studies of the Cosmic Microwave Background (CMB) by Planck combined with bayon acoustic oscillations (BAO) measurements [14]:

$$N_{eff} = 2.99^{+0.34}_{-0.33}. \tag{21}$$

Various different assumptions about the history of the universe can be made and different data sets can be chosen to obtain slightly different results [9] — for the purposes of this exploratory work, wading through this landscape is unnecessary.

For fully decoupled sectors that never enters (or reenters) thermal equilibrium with our sector, we obtain additional contributions to N_{eff}^{SM} [9]

$$\Delta N_{eff} = \frac{4}{7}\left(\frac{11}{4}\right)^{4/3} g_h \xi_h^4. \tag{22}$$

Here, g_h represents the effective number of relativistic degrees of freedom for the hidden sector when the hidden sector has a temperature $T_h = \xi_h T_\gamma$. Contours for Eq. (22) at various temperature ratios as well as CMB bounds are plotted in Fig. V. We take this approach and generalize it to include many additional sectors:

$$\Delta N_{eff} = \sum_i \frac{4}{7}\left(\frac{11}{4}\right)^{4/3} g_i \xi_i^4. \tag{23}$$

As Fig. V demonstrates, sectors with a temperature ratio above $\xi_h \sim 0.5$ with even a couple of relativist particles are immediately excluded by CMB constraints. Accordingly, the additional sectors present in this project must be heated to a much smaller fraction of our own sector's temperature.

A. Exotic Sector Contributions

The original Nnaturalness paper focused on the (stronger) N_{eff} constraints from the additional standard sectors and ignored the exotic sectors altogether [2]; in contrast, we take the opposite approach. Since we're more interested in a more general scenario with multiple dark phase transitions, we focus in on whether zero vev sectors can dodge these N_{eff} bounds.

Within the framework of SM-like particle content (save the higgs mass parameter), our exotic sectors feature at most 106.75 effective degrees of freedom at high energies: 72 from quarks, 12 from charged leptons, 6 from neutrinos, 16 from gluons, 2 from photons, 6 from W bosons (no longitudinal modes due to a no symmetry breaking), 4 from the higgs sector (again, no symmetry breaking leads to 3 additional modes), for a total of 118 degress of freedom. Scaling the fermionic contributions by 7/8 gives us 106.75 effective relativistic degrees of freedom. After the higgses freeze out, 4 degrees of freedom are lost; when the QCD phase transition occurs 35 bosonic degrees of freedom are gained while 72 fermionic are lost, leaving 56.75 effective degrees of freedom. Since all additional sectors are colder than our own by the time photon

decoupling occurs ($\sim 0.39\,\mathrm{eV}$), the pions of all of these sectors will, in accordance with Eq. (19), have a much higher mass than the sector temperature and thus will have frozen out long before — leaving at most 11.25 effective degrees of freedom per sector.

Coupling the number of effective degrees of freedom per sector with the energy density scaling of $\sim 1/m_H^4$ found in the zero vev sectors leads to tiny temperature ratios. Assuming a reheating temperature of 100 GeV and a completely uniform distribution of sectors, the temperature of the first exotic sector is slightly more than 6% of our sector at reheating. Applying Eq. (23) to this particular situation gives us:

$$\Delta N_{eff} = \sum_i \frac{4}{7}\left(\frac{11}{4}\right)^{4/3} g_i \left(\frac{0.06}{i^2}\right)^4. \tag{24}$$

Summing over all sectors (sectors above $i \sim 10$ essentially don't contribute due to the small temperature ratios) gives us a contribution of $\mathcal{O}(10^{-4})$. Evolving the sectors thermal histories forward in time to the recombination era gives us a slightly larger value, but still of order $\mathcal{O}(10^{-4})$; well under current CMB bounds.

It should be noted that modifying the exotic sectors' structure (e.g. adjusting the exotic sectors to have a lower higgs mass squared or clustering multiple hidden sectors close to the first exotic one) leads to a ΔN_{eff} contribution that is larger than the base Nnaturalness case. This increase is not excluded by current bounds, indicating a large degree of liberty in the structure and number of exotic hidden sectors.

B. High Scale Transitions

The generalization of possible reheating mechanisms mentioned in section III — where the reheating mechanism no longer depends on the higgs' mass parameter of a given sector — opens up a wide range of hidden sectors for study. Specifically, this allow mirror sectors with large vevs to reheat to significant energy densities and thus produce gravitational waves with enough power to be detected. Crucially, despite this analysis being limited to mirror sectors with large higgs' masses this analysis pertains to any strong, confining phase transition at high scales.

Since N_{eff} constraints remain our strongest cosmological bounds for massive standard sectors, our starting point for exploring the limits of high transition temperatures is Eq. (23). Assuming heavy, standard sectors we can saturate the bounds of Eq. (21) and solve for the maximum energy density allowed for any number of sectors:

$$\begin{aligned} &\rho_i \sim 0.25\rho_{SM} && \text{1 hidden sector,}\\ &\rho_i \sim 0.17\rho_{SM} && \text{5 hidden sectors,}\\ &\rho_i \sim 0.14\rho_{SM} && \text{10 hidden sectors,}\\ &\rho_i \sim 0.08\rho_{SM} && \text{100 hidden sectors.} \end{aligned} \tag{25}$$

Using these restrictions, we can examine the behaviour of standard sectors with a much larger vev than our own. In terms of the Nnaturalness framework, this consisted of looking at various different sectors above the critical index, as mentioned in Sec. IV. The signals for both the maximal case (10^{16} limit) and several other high transition temperatures (involving sectors $i > 10^{10}$) scenarios are shown in Sec. VI.

VI. SIGNALS

Gravitational waves are produced with contributions from different components of the SFOPT's evolution. The three leading order contributions to the GW power spectrum are as follows:

- **Scalar field contributions** Ω_ϕ: Caused by collisions of the bubble walls, the solutions being completely dependent on the scalar field configuration. With efficiency factor $\kappa_\phi = 1 - \alpha_\infty/\alpha$.
- **Sound wave contributions** Ω_v: Sound waves within the plasma after bubble collision will produce β/H enhanced gravitational waves. With efficiency factor $\kappa_v \propto \alpha_\infty/\alpha$.
- **Magnetohydrodynamics contributions** Ω_B: MTG shocks within the plasma, left over from the sound wave propagation, will produce gravitational waves. With efficiency factor $\kappa_{turb} \approx 0.1\kappa_v$.

The total gravitational wave power spectrum is a linear combination of the three contributions,

$$h^2\Omega_{GW} \approx h^2\Omega_\phi + h^2\Omega_v + h^2\Omega_{turb} \tag{26}$$

In essence, this is a linear combination of the individual spectral shapes weighted by their efficiency factors κ. As shown in section IV, the mass spectrum from the dark QCD chiral breaking sectors is such that the runaway bubble condition is satisfied ($\alpha > \alpha_\infty$). In this case, the efficiency factors for sound wave and MHD contributions tend to zero and the GWs produced are purely from bubble collisions, $h^2\Omega_{GW} \approx h^2\Omega_\phi$. The form of the GW power spectrum at the time of nucleation is given as,

$$h^2\Omega_{GW} = 7.7\times 10^{-2}\left(\frac{\kappa_\phi \alpha}{1+\alpha}\right)^2\left(\frac{H}{\beta}\right)^2 S(f) \tag{27}$$

Where we have assumed an optimistic bubble wall velocity of $v \sim c$ for runaway bubbles. $S(f)$ is the frequency spectrum, and a parametric from has been found through numerical simulations of bubble wall collisions.

$$S(f) = \frac{3.8\,(f/f_p)^{2.8}}{1 + 2.8\,(f/f_p)^{3.8}} \tag{28}$$

The peak frequency, f_p is a function of the temperature of the SM at the time of nucleation. Depending on the

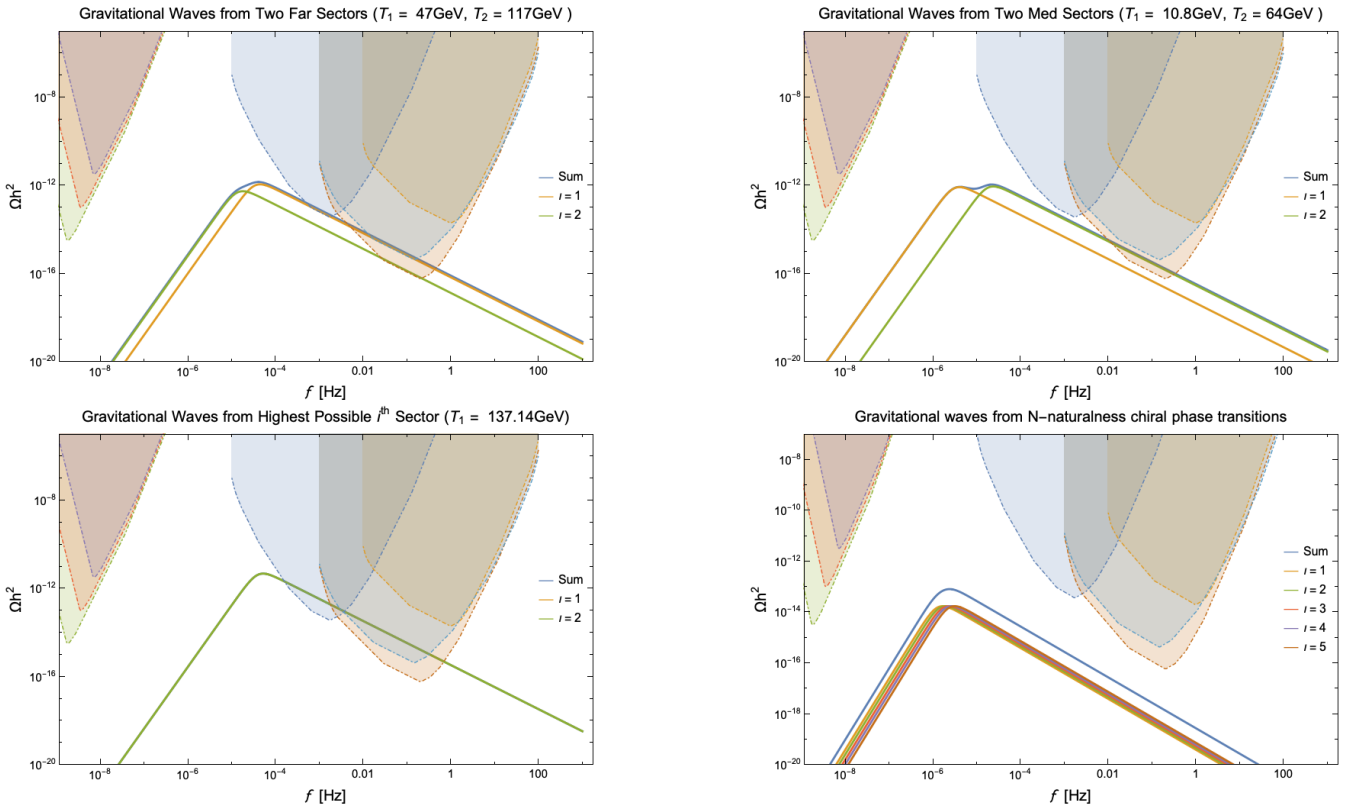

FIG. 4. Gravitational wave power spectrum for various models. The top row consists of two models with only two hidden sectors undergoing SFOPT at differing temperatures. The bottom right (left) are examples of exotic sectors, discussed in section V, with sectors reheated at $\rho \sim 0.25\rho_{SM}$ ($\rho \sim 0.17\rho_{SM}$). All contributions are assumed to be purely from bubble collisions Ω_ϕ, with $\beta/H = 10$. The shaded curves are the power law noise curves calculated from expected sensitivity curves for space-based interferometers and pulsar timing arrays; Lisa (blue), DECIGO (light blue), BBO (red), SKA 5-year (purple), SKA 10-year (orange), SKA 20-year (green)

model, the various hidden sectors can phase transition at different scales and therefore temperatures, cause a shift in the GW spectrum's peak frequency given by,

$$f_p = 3.8 \times 10^{-8}\,\mathrm{Hz}\left(\frac{\beta}{H}\right)\left(\frac{T_\gamma}{100\,\mathrm{GeV}}\right)\left(\frac{g_*}{100}\right)^{\frac{1}{6}} \tag{29}$$

Now that the framework has been laid out for the creation of GW from a single SFOPT, we generalize to multiple sectors going under independent, coherent SFOPT. In the models presented in this paper, we consider a subset of N-hidden sectors that phase transition at a SM temperature of T_γ^i. As the GWs propagate in free space, the energy density and frequency spectrum, at the time of production $\Omega^*_{GW}(f)$, will redshift to today's value $\Omega^0_{GW}(f) = \mathcal{A}\,\Omega^*_{GW}((a_0/a)f)$. Assuming that the sectors are completely decoupled before and after their respective SFOPT, the total GW power spectrum that would be measured today is given by the coherent sum,

$$\Omega^0_{GW} = \sum_i^N \mathcal{A}^i\,\Omega^{i,*}_{GW}((a_0/a)_i f) \tag{30}$$

It is safe to assume that a subset of parameters of the SFOPT do not differ between sectors within Nnatrualness or other decoupled hidden sector models. In the case of N-copies of dark QCD-like phase transitions, the relativistic degrees of freedom, phase transition rate, the dark QCD scale, are all similar. This makes the redshifting factor, $\mathcal{A}^i$, independent of sector number. We can also see that the frequency dependence in the spectrum takes the form of f/f_p, this causes a cancellation of the redshifting factors in the ratios. As multiple sectors phase transition at different times, and therefore temperatures, the peaks will shift relative to each other, purely from the linear temperature dependence of the peak frequency $f_p \sim T_\gamma$. This is seen in figures [], where the spectrum peaks are shifted causing a peak broadening of the convoluted spectrum. The broadening can be substantial if the hidden sectors transition between a large gap of time (temperature). Eventually, a temperature limit will be reached at which two (or multiple) peaks, if the amplitudes are comparable.

VII. CONCLUSION

[1] P. Schwaller, Phys. Rev. Lett. **115**, 181101 (2015), arXiv:1504.07263 [hep-ph].

[2] N. Arkani-Hamed, T. Cohen, R. T. D'Agnolo, A. Hook, H. D. Kim, and D. Pinner, Phys. Rev. Lett. **117**, 251801 (2016), arXiv:1607.06821 [hep-ph].

[3] F. Cuteri, C. Czaban, O. Philipsen, and A. Sciarra, *Proceedings, 35th International Symposium on Lattice Field Theory (Lattice 2017): Granada, Spain, June 18-24, 2017*, EPJ Web Conf. **175**, 07032 (2018), arXiv:1710.09304 [hep-lat].

[4] B. Svetitsky and L. G. Yaffe, Nuclear Physics B **210**, 423 (1982).

[5] R. D. Pisarski and F. Wilczek, Phys. Rev. **D29**, 338 (1984).

[6] J.-W. Cui, H.-J. He, L.-C. Lu, and F.-R. Yin, Phys. Rev. **D85**, 096003 (2012), arXiv:1110.6893 [hep-ph].

[7] M. Tanabashi *et al.* (Particle Data Group), Phys. Rev. D **98**, 030001 (2018).

[8] M. E. Peskin and D. V. Schroeder, *An Introduction to quantum field theory* (Addison-Wesley, Reading, USA, 1995).

[9] M. Breitbach, J. Kopp, E. Madge, T. Opferkuch, and P. Schwaller, (2018), arXiv:1811.11175 [hep-ph].

[10] C. Caprini *et al.*, JCAP **1604**, 001 (2016), arXiv:1512.06239 [astro-ph.CO].

[11] J. R. Espinosa, T. Konstandin, J. M. No, and G. Servant, JCAP **1006**, 028 (2010), arXiv:1004.4187 [hep-ph].

[12] M. D. Schwartz, *Quantum Field Theory and the Standard Model* (Cambridge University Press, 2014).

[13] G. Mangano, G. Miele, S. Pastor, T. Pinto, O. Pisanti, and P. D. Serpico, Nucl. Phys. **B729**, 221 (2005), arXiv:hep-ph/0506164 [hep-ph].

[14] N. Aghanim *et al.* (Planck), (2018), arXiv:1807.06209 [astro-ph.CO].